Catalysis Science & Technology

Accepted Manuscript

ROYAL SOCIETY OF CHEMISTRY

www.rsc.org/catalysis

Journal Name

RSCPublishing

ARTICLE

Microwave-assisted synthesis of plate-like SAPO-34 nanocrystals with increased catalyst lifetime in the methanol-to-olefins reaction

Cite this: DOI: 10.1039/x0xx00000x

T. Álvaro-Muñoz,[a] E. Sastre,[a] C. Márquez-Álvarez[a]

Received ooth January 2012,
Accepted ooth January 2012

DOI: 10.1039/x0xx00000x

www.rsc.org/

Nanocrystalline SAPO-34 catalysts were obtained using microwave-assisted hydrothermal synthesis. Compared to conventional heating, the use of microwave irradiation allowed to shorten crystallization time from days to several hours, caused lower level of silicon incorporation, which led to slightly lower acidity, and modified crystal size and morphology. SAPO-34 catalyst synthesized in microwave oven exhibited longer lifetime in the methanol-to-olefins reaction due to their thin plate-like crystal morphology, which facilitates accessibility of the reactant to the acid sites.

Introduction

Low olefins such as ethylene, propylene and butene have been widely used as raw materials of polyolefins and as the starting materials for various chemicals in the petrochemical industry.[1] Alternative routes for the production of light olefins, among other important petrochemical products, are more attractive than ever before due to the rapid increase in the price of crude oil and its shortage in the foreseeable future.[2,3] The methanol to olefins (MTO) process has proven to be the most successful non-petrochemical route for the production of light olefins from the abundant resources of natural gas or coal.[4] Methanol can be efficiently produced from syngas obtained by natural gas reforming or carbon gasification.[5-7] Also, it might even provide an environmentally carbon neutral alternative to fossil carbon sources[8] if produced by chemical recycling of carbon dioxide via hydrogenation[9] or from syngas obtained by biomass gasification.[10] This reaction is efficiently catalyzed by various solid acids. The conversion of methanol over medium-pore zeolites (such as ZSM-5) normally produces extensive amounts of aromatics and paraffins (MTG process) and, in the case of large-pore zeolites, rapid coke formation.[11-13] On the contrary, small-pore molecular sieves generate higher proportion of C2-C4 olefins, due to the diffusion properties and dimensions of the cavities of zeolitic materials. However, the porous structure is not the only factor that determines the high selectivity to C2-C4 olefins, as high selectivities to light paraffins (mainly propane) can also be obtained with small-pore size zeolites. Decreasing the concentration of strong acid sites, which are responsible for hydrogen transfer reactions, is a key factor in reducing the conversion of olefins into paraffins. The methods used to reduce the concentration of strong acid sites on zeolites (and thus avoid these hydrogen transfer reactions) are dealumination, cation exchange and isomorphous substitution of aluminium by other trivalent cations.

Silicoaluminophosphate materials (SAPO) have a mild acidity and, therefore, they represent a very interesting alternative to obtain high selectivity towards light olefins in the MTO process. Zeolite-type small-pore microporous silicoaluminophosphate SAPO-34 has been proven an excellent catalyst for the MTO process, showing exceptionally high selectivity to lower olefins. SAPO-34 has the zeolite chabazite framework topology (framework code CHA), characterized by elongated cavities interconnected by 8-ring windows with a pore diameter of 0.38 nm. This catalyst has the advantage of a high selectivity toward light olefins at nearly 100% conversion of methanol, but it shows rapid deactivation. Previous studies revealed that deactivation of catalysts in the MTO process occurs mainly due to mass transfer limitation associated to coke deposition.[14-16] Several strategies have been considered to prolong the lifetime of the catalyst in the MTO reaction, such as modifying the zeolite pore structure and acidity. Besides, catalysts with small crystallite size showed the advantage of enhanced mass transfer properties and reduction in coke formation.[17]

The morphology of SAPO-34 crystals can affect their properties and applications and various methods have been suggested to improve catalyst lifetime in the MTO reaction.[18-24] The catalyst deactivation may be strongly correlated with the particle size due to the diffusion limitations of the guest molecules in the micropores.[25] For large catalyst crystals, residence time for hydrocarbons is high because of the long diffusion path. Aromatic compounds cannot escape from the pores of SAPO-34 and successive polymerizations readily occur because of the long reaction time. Several studies

examined the effect of the crystal size of SAPO-34 on its selectivity and deactivation in the MTO reaction. In large crystals, the reactions were controlled by limitations on the diffusion of methanol and the intermediate product dimethyl ether (DME), while SAPO-34 with a crystal size of less than 500 nm showed much longer lifetime in the MTO reaction.[18,21] It was concluded that deactivation is related to diffusion limitation and that catalysts with smaller crystal size show slower deactivation due to the higher proportion of accessible cages near the external surface. The short diffusion length in nanoscale crystals, resulting in the reduction of residence time of reactant and products of MTO reactions, was claimed to explain their longer catalyst lifetime.[15] The increase in the number of accessible cages near the external surface for nanocrystalline SAPO-34 catalyst was proved very efficient in improving methanol conversion.[21,25]

During the past decade, considerable attention has been given to the fabrication of nanomaterials.[26,27] As discussed by many researchers, the synthesis of AlPOs, zeolites and other porous materials via microwave heating has overcome many of the drawbacks found for conventional heating of the synthesis gels in a convection oven. The microwave technique presents several advantages compared with conventional hydrothermal synthesis such as homogenous nucleation, which gives smaller and uniform-size formation of crystals with rather large external surface areas, rapid crystallization rates, phase-controlled synthesis, facile morphology control and greener synthesis as it is an energy efficient way of heating.[28-32]

Microwave heating, which has been demonstrated to influence reaction kinetics and selectivity in chemical processes, is becoming an increasingly important tool in the synthesis of nanoporous materials. It may overcome typical problems that can be related to the synthesis of zeolites such as poor reproducibility of the process, impurity of the nanoporous structure, need of large amount of mineralizing agents and water, long crystallization time, etc. It was in 1988 when Mobil researchers proved the effectiveness of microwave energy for synthesizing zeolites.[33] Since that report, microwave-assisted synthesis has been considered a promising method because it is generally quite faster, cleaner, simpler and more energy efficient than the conventional methods.[34] Up to date, several zeolitic materials have been synthesized using microwave irradiation such as zeolites A,[33,35] X,[35] Y,[36] ZSM-5,[35,36] beta,[37] TS-1[38] and TS-2,[39] as well as AlPO-type materials like AlPO-5[40,41] and VPI-5.[42]

The microwave method has been mainly focused on substantial reduction in crystallization time.[36,43-45] However, in addition to the shortening of synthesis time, the microwave technique may provide an efficient way to control particle size distribution, crystalline phase and macroscopic morphology, and to enhance mesoporosity in the synthesis of nanostructured materials.[46,47,48]

In the present work, we report on the preparation of SAPO-34 using very dilute zeotype precursor solutions[49] and microwave irradiation in order to obtain nanocrystalline materials. The products were characterized by different physicochemical techniques and tested in the MTO reaction. These results are compared to those obtained using the conventional hydrothermal method. Our study demonstrates the remarkably enhanced lifetime of nanosized SAPO-34 catalyst in the MTO reaction.

Experimental

Synthesis of SAPO-34 molecular sieves

Hydrothermal synthesis of SAPO-34 samples was carried out using tetraethylammonium hydroxide (TEAOH, Sigma-Aldrich, 35 wt% in water) as template and aluminium chloride (Sigma Aldrich, 99%) as aluminium source. Two different sources of silicon were used: colloidal silica (Ludox SM-30, 30% in water) and tetraethylorthosilicate (TEOS, Merck 98%). The gel composition was: $1Al_2O_3$: $1P_2O_5$: $0.6SiO_2$: 6TEAOH: $110H_2O$ (Table 1). The synthesis to get pure SAPO-34 was realized according to the method published previously.[49] The gel obtained was transferred into teflon-lined autoclaves with a capacity of 100 cm^3, and heated at 423K either statically or with magnetic stirring under autogeneous pressure in a Milestone ETHOS One Microwave Labstation during different periods of time. The resulting solids were collected by centrifugation, washed with water and ethanol and dried at room temperature overnight. The organic template and the water trapped within the micropores of the as-synthesized solids were removed by calcination at 823 K prior to catalyst testing.

Characterization

Powder X-ray diffraction (XRD) patterns of as-synthesized and calcined samples were recorded on a PANalytical X´Pert diffractometer using CuK_α radiation with a nickel filter. The textural data (Pore volume and BET surface area) were determined by nitrogen adsorption measurement using a Micrometrics ASAP 2010 volumetric apparatus. Previous to measure the nitrogen adsorption/desorption isotherms at 77 K, samples were degassed at 623 K under vacuum for at least 20 hours. The crystal size and morphology were analysed by scanning electron microscopy (SEM) using a Philips XL30 microscope operating at 20 kV.

The organic content of the samples was studied by elemental analysis with a Perkin-Elmer 2400 CHN analyser and by thermogravimetric analysis (TGA) using a Perkin-Elmer TGA7 instrument. TG analyses were carried out at a heating rate of 20 K/min under air flow. Elemental analysis for Al, P and Si in calcined samples was performed by inductively coupled plasma optical emission spectrometry (ICP-OES, Perkin-Elmer 3300DV instrument) after sample dissolution by alkaline fusion.

Ammonia temperature-programmed desorption (NH_3-TPD) was performed using a Quantachrome ChemBET-3000 TPR/TPD equipment. Typically, 100 mg of sample pellets (20–40 mesh) were pre-treated at 823 K for 1 h in helium flow (25 mL/min) and subsequently cooled to the adsorption temperature (400 K). A gas mixture of 5.0 vol. % NH_3 in He was then allowed to

Journal Name RSCPublishing

ARTICLE

Table 1 Synthesis conditions used to obtain SAPO-34 materials from gels with molar composition Al_2O_3 : P_2O_5 : 0.6 SiO_2 : 6 TEAOH : 110 H_2O heated in microwave oven at a crystallization temperature of 423 K.

Sample	x	Silicon source	Stirring	pH gel	pH cryst.[b]	Time (hours)	Product
MW-0.6L-7s	0.6	LUDOX	YES		7.84	7	Amorphous
MW-0.6L-8s	0.6	LUDOX	YES		7.79	8	CHA
MW-0.6L-10s	0.6	LUDOX	YES		7.89	10	CHA
MW-0.6L-15s	0.6	LUDOX	YES		8.09	15	CHA
MW-0.6L-20s	0.6	LUDOX	YES	7.95	8.22	20	CHA
MW-0.6L-7	0.6	LUDOX	NO		7.93	7	Amorphous
MW-0.6L-8	0.6	LUDOX	NO		7.77	8	CHA+Amorphous
MW-0.6L-10	0.6	LUDOX	NO		8.04	10	CHA
MW-0.6L-15	0.6	LUDOX	NO		8.12	15	CHA
MW-0.6L-20	0.6	LUDOX	NO		8.63	20	CHA
MW-0.6T-8s	0.6	TEOS	YES		6.77	8	Amorphous
MW-0.6T-10s	0.6	TEOS	YES		6.58	10	Amorphous
MW-0.6T-15s	0.6	TEOS	YES		7.88	15	CHA+Amorphous
MW-0.6T-20s	0.6	TEOS	YES	7.86	7.80	20	CHA
MW-0.6T-8	0.6	TEOS	NO		6.79	8	Amorphous
MW-0.6T-10	0.6	TEOS	NO		6.11	10	CHA+Amorphous
MW-0.6T-15	0.6	TEOS	NO		7.80	15	CHA
MW-0.6T-20	0.6	TEOS	NO		7.91	20	CHA
O-0.6L[a]	0.6	LUDOX	NO	8.5	9.3	120	CHA
O-0.6T[a]	0.6	TEOS	NO	8.5	8.4	120	CHA

[a]Reference samples obtained by heating the gel in a convection oven.
[b]pH of the gel before it was introduced in the autoclaves.

flow over the sample for 4 h at a rate of 15 mL/min followed by helium flow for 30 min to remove weakly adsorbed NH_3.

Catalyst testing

Methanol conversion to olefins was tested at 623, 673 and 723 K in a PID Eng&Tech Microactivity-Reference automated compact microreactor with a continuous down flow packed bed reactor made of glass operating at atmospheric pressure. Catalyst weight (1.0 g; 20-30 mesh pellets size) and methanol flow rate (0.100 ml/min) were adjusted in order to obtain a weight hourly space velocity (WHSV) of 1.2 h^{-1}. Previous to the reaction, samples were pre-treated under nitrogen flow at 723 K for 1 hour. During the reaction, nitrogen was used as an inert diluent gas and co-fed with methanol into the reactor with a constant methanol/nitrogen mol ratio of 1/1. Methanol was fed as liquid using a Gilson 307 HPLC pump, vaporized and mixed with the nitrogen stream in a pre-heater set at 473 K. The reaction products were analysed on-line by gas chromatography using a Varian CP3800 gas chromatograph equipped with flame ionization (FID) and thermal conductivity (TCD) detectors, with a Petrocol DH50.2 capillary column and a Porapack Q 80-100 mesh packed column for separation of hydrocarbons and oxygenates, respectively.

Finally, a 25 mL/min helium flow was passed over the sample while increasing the temperature to 823 K at a rate of 10 K/min.

Results and discussion

Crystal structure and morphology analysis

X-ray powder diffraction patterns of as-synthesized samples (Fig. S1 in Supplementary Information) show that materials obtained from gels with a Si/(Al+P) atomic ratio of 0.15, using either Ludox or TEOS as silicon source, possess the SAPO-34 structure (CHA). The diffractograms of samples obtained after 7 h of microwave heating of gels prepared with colloidal silica (Ludox) indicate that the solids were essentially amorphous, although several very weak peaks were detected that might be assigned to the most intense CHA reflections. At a crystallization time of 8 h, patterns characteristic of the CHA structure[49] are observed. The peaks intensities were higher for the sample obtained with stirring, which indicates that stirring of the gels during the hydrothermal synthesis increased slightly the crystallization rate. Nevertheless, all the samples collected after 10 h of microwave heating showed the maximum crystallinity and the intensity of the diffraction peaks remained

constant for longer crystallization times, both for static and stirred syntheses.

Samples synthesized using TEOS as silicon source had slower crystallization rate. The diffractograms show that solids obtained at 8 h were amorphous and after 10 h of static synthesis conditions only weak reflections corresponding to the CHA phase are observed. Materials with high crystallinity were obtained after 15 and 20 h of static synthesis. Lower crystallization rate was observed when the syntheses were carried out under stirring, as the solid obtained after 10 h was amorphous and samples obtained after 15 and 20 h showed lower crystallinity than their counterparts obtained via static synthesis. Nevertheless, the crystallization of the CHA phase was significantly enhanced using microwave irradiation respect to the conventional heating method, for up to 5 days were required to crystallize SAPO-34 when the syntheses were carried out using similar gel composition in a convection oven.[49]

XRD patterns of samples obtained after 20 hours of microwave irradiation and 5 days of synthesis in convection oven are shown in Fig. 1. Some differences in peak width and relative intensities can be observed among patterns, which suggests that the samples have different particle size or morphology. This was confirmed by SEM analysis (Fig. 2). Samples obtained by thermal treatment of gels in convection oven had crystals with a rhombohedral habit and relatively uniform size in the 200-300 nm range, regardless of the silicon source used. In contrast, the syntheses carried out using microwave irradiation led to the growth of plate-like crystals, with only a few tenths of nm thickness. In the case of the sample prepared from TEOS and crystallized under stirring, SEM images show spherical aggregates of nano-sized crystals.

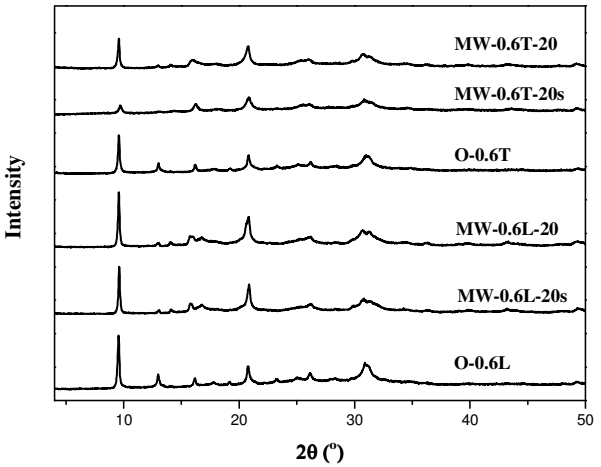

Fig. 1 XRD patterns of as-synthesized samples.

Textural Properties

Calcined materials were analysed by nitrogen adsorption-desorption at 77 K in order to determine their textural properties. All the samples present type I isotherms (according to the IUPAC classification,[50] corresponding to microporous materials, with an additional nitrogen uptake at high relative pressure due to filling of interparticle spaces in the mesopore-size range (Fig. S2 in Supplementary Information). Data of pore volume and surface area calculated from the isotherms are collected in Table 2. It is necessary to consider that it is commonly accepted that this technique is not the most appropriate way to determine unambiguously the surface and pore volume of small pore materials like SAPO-34, and it should be used only for comparative purposes. It can be observed that samples prepared under microwave irradiation have lower values of surface area and pore volume than those synthesized in convection oven. This is mainly associated to a smaller microporous component in the samples prepared in the microwave oven, for the values of external surface area and pore volumne are very similar among all the samples. In particular, the sample obtained from TEOS at 20 h of microwave irradiation under stirring exhibits significantly low microporosity. This result can be attributed to a low crystallinity of this sample, as suggested by the weak intensity of diffraction peaks observed in its XRD pattern (Fig. 1).

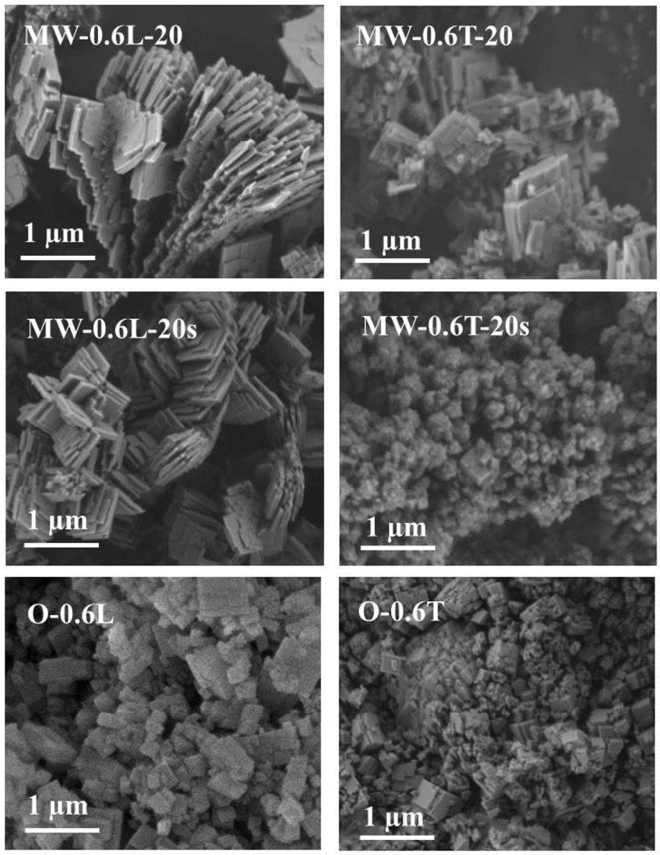

Fig. 2 SEM images of calcined samples.

Thermogravimetric and Elemental Analysis

Thermogravimetric analyses (TGA) were performed aiming to verify the incorporation of the SDA molecules in the structure of the as-made samples and their subsequent complete elimination after calcination prior to the use of SAPO-34 materials in the catalytic reactions. The TGA profiles of selected as-synthesized samples are plotted in Fig. 3. For all

samples, a first weight loss occurs at temperatures below 450 K (step I), which can be attributed to desorption of adsorbed water molecules. At higher temperatures, decomposition and combustion of organic species contained inside the pores of the structure takes place. Template removal is nearly complete in the temperature range 450-800 K. This process takes place in several steps, which leads to a number of peaks in the derivative curves. It is worth noting that the samples obtained by each one of the two heating methods employed show very different weight loss profiles associated to removal of the organic species. In the case of samples prepared in the microwave oven, template removal starts at a temperature as low as 450 K. The TGA profiles of those samples show a weight loss step in the temperature range 450-550 K (step II), which is the most intense for samples prepared with TEOS. Subsequently, a more progressive weight loss takes place between 550 and 800 K (step III). In contrast, for samples synthesized in the convection oven, a nearly constant weight is observed in the temperature range 450-550 K and the removal of template occurs mainly at temperatures around 750 K. An additional small weight loss is observed at temperatures higher than 800 K (step IV), particularly in the case of samples synthesized with Ludox. This might be attributed mainly to the removal of organic residues occluded in the channels and cages of SAPO-34, although it should be noticed that dehydroxylation processes might contribute to the weight loss observed.

Table 2 Textural properties of selected calcined samples of SAPO-34.

	Surface area (m^2/g)			Pore volume (cm^3/g)		
Sample	S_{BET}	S_{micro}	S_{ext}	V_{tot}	V_{micro}	V_{ext}
MW-0.6L-20s	339	295	44	0.28	0.12	0.16
MW-0.6L-20	482	448	33	0.35	0.19	0.16
MW-0.6T-20s	176	125	51	0.19	0.05	0.14
MW-0.6T-20	418	342	76	0.33	0.14	0.19
O-0.6L	619	588	31	0.42	0.25	0.17
O-0.6T	633	558	76	0.59	0.23	0.36

The TGA profiles shown in Fig. 3 reveal that the decomposition and combustion of the template occurs in a different way for the different samples. While for samples prepared in the oven the template removal process is associated mainly to a single step centred at 750 K, samples prepared in the microwave oven show, at least, two different steps of template removal ranging from 450 K to ca. 800 K. The fact that the template decomposition began at lower temperature in these samples suggests that some amount of TEAOH is bonded to the inorganic network by weaker bonds and a lower temperature is necessary for its removal. These differences are most noticeable in samples prepared with TEOS under microwave irradiation, for which most of the organic is removed at temperatures below 600 K.

The percentage of weight losses determined in every step and the corresponding amount of organic estimated for every sample (calculated from weight loss of steps II to IV) are presented in Table 3. The estimated organic contents are in good agreement with results obtained from CHN elemental analyses (Table 4), which supports the previous weight losses assignment. Moreover, the experimental C/N ratios determined for the different samples were close to 8, the value corresponding to tetraethylammonium cation. This represents an additional evidence of the incorporation of the SDA into the zeolitic structure. Based on the topological structure of the SAPO-34 molecular sieve, the average number of template molecules per cage in the different samples was calculated (Table 4). For all the samples prepared with colloidal silica, the estimated organic content corresponds to one molecule of SDA (TEAOH) incorporated per unit cell of SAPO-34. However, samples synthesized with TEOS contain 2 and up to 3 molecules of ADE per unit cell. As only one TEA^+ cation can occupy the cage of SAPO-34 and the unit cell contains a single cage, the results indicate that there are organic species in excess that should be located on the external surface of the crystals.

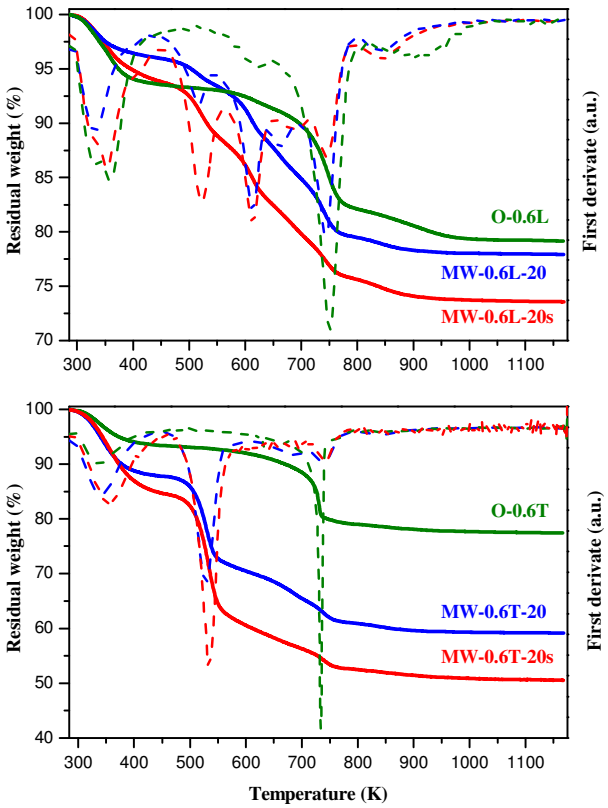

Fig. 3 Thermogravimetric profiles (solid lines) and first derivative (dashed lines) of as-synthesized SAPO-34 samples.

The chemical composition of samples determined by ICP-OES is presented in Table 5. The Si/(Al+P) ratios of the solids obtained in the microwave oven are substantially lower than that of the starting gel. In samples prepared with TEOS using microwave irradiation the silicon incorporation is slightly higher than in samples synthesized with colloidal silica. Nevertheless, all these sample show lower levels of silicon incorporation than samples prepared in the convection oven,

which possess the same Si/(Al+P) ratio than their synthesis gels.

Table 3 Thermogravimetric analyses of selected samples of SAPO-34.

Sample	Weight loss (%) I <450K	II 450-550K	III 550-800K	IV >800K	weight ratio[a]
MW-0.6L-20s	6.2	5.7	12.3	2.2	0.22
MW-0.6L-20	4.0	2.5	14.0	1.6	0.19
MW-0.6T-20s	15.6	25.1	6.7	2.1	0.40
MW-0.6T-20	12.3	17.0	9.8	1.8	0.33
O-0.6L	6.4	-	11.5	2.8	0.15
O-0.6T	6.7	-	14.4	1.4	0.17

[a]Estimated total organic content per unit mass of SAPO inorganic material.

Table 4 Organic content of the samples.

Sample	C	H	N	C/N	% organic	moles of ADE/u.c
MW-0.6L-20s	12.23	3.51	1.79	7.99	17.53	1.27
MW-0.6L-20	11.24	3.00	1.65	7.97	15.89	1.10
MW-0.6T-20s	20.69	5.94	2.99	8.08	29.61	3.09
MW-0.6T-20	17.65	4.85	2.57	8.03	25.06	2.27
O-0.6L	9.89	2.84	1.59	7.26	14.32	1.07
O-0.6T	10.09	2.93	1.61	7.31	14.63	1.06

Characterization of acidity

The acidity of the catalysts has been evaluated by TPD of ammonia (Fig. 4 and Table 5). The area under the TPD profile indicates the total amount of ammonia desorbed, which is proportional to the total acidity, whereas the desorption temperature indicates the acid strength of the sites, as the stronger the acid sites the higher the required desorption temperature.

Table 5 Chemical analyses and acidity measurements of selected SAPO-34 samples.

Sample	Si/(Al+P) solid	Si incorporationa	mmol NH_3/g
MW-0.6L-20s	0.05	0.38	0.37
MW-0.6L-20	0.06	0.38	0.44
MW-0.6T-20s	0.08	0.54	0.39
MW-0.6T-20	0.09	0.61	0.41
O-0.6L	0.15	1.00	0.64
O-0.6T	0.15	1.00	0.67

[a]The level of silicon incorporation is defined as the ratio between the atomic fraction of Si in the solid and that in the gel: $[Si/(Si+Al+P)]_{solid}$ /$[Si/(Si+Al+P)]_{gel}$

In the case of samples prepared with Ludox, the materials show a similar profile. All of them present a major desorption peak at low temperature (with a maximum around 515K) which is an indication of site uniformity and of a relatively weak acid strength. The TPD profile shows some tailing towards higher temperatures, indicating the presence of a small proportion of acid sites with higher strength. This tailing is more predominant in sample prepared in the oven O-0.6L. However, samples prepared with TEOS present different TPD profiles. In the case of materials prepared in the microwave it is observed a major desorption peak at low temperature (with a maximum around 520K) which is an indication of site uniformity and of a relatively weak acid strength, similar to materials prepared with Ludox. However, sample O-0.6T exhibits a broader desorption profile, showing an important contribution of a desorption band with maximum at around 610 K, corresponding to strong acid sites, overlapping with the low temperature ammonia desorption peak attributed to weak acid sites. It is important to remark that using both sources of silicon, the total amount of acid sites of samples synthesized in the convection oven is higher than in the case of samples synthesized using microwave irradiation (Table 5). This result correlates with the higher silicon content of the former samples.

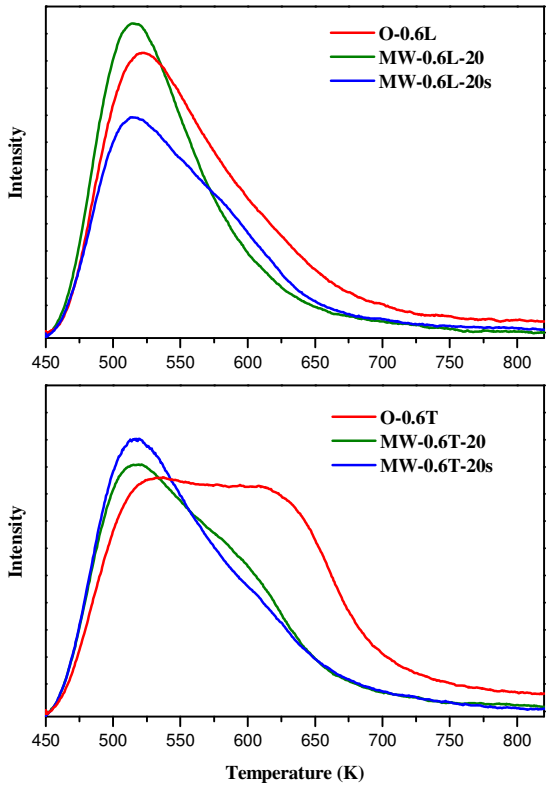

Fig. 4 NH3-TPD plots of calcined SAPO-34 catalysts.

Catalytic Activity

The catalytic activity of these materials in the MTO reaction was studied at 623, 673 and 723 K and WHSV of 1.2 h^{-1} as it has been described previously in the experimental section. The conversion level and selectivity to light olefins (C2-C4) are presented as a function of time on stream in Fig. 5 and 6. For tests carried out at 623K, lifetime of all the catalyst was very low. The rapid deactivation indicates that these catalysts possess a relatively low amount of acid sites with the high strength required to catalyse the conversion of methanol and the intermediate dimethylether (DME) to hydrocarbons at this low

temperature. At higher reaction temperatures, the catalyst lifetime increased notably, as acid sites of lower strength would be active to continue the transformation of DME to light olefins at 673 and 723 K. However, at the highest reaction temperature (723 K), all the catalysts show faster deactivation than at 673 K, showing an enhancement of the formation of heavier hydrocarbon products that cause pore-blocking, making the active sites of the catalyst less accessible for reactant molecules.

For both silicon sources (Ludox and TEOS), the catalysts prepared in microwave oven under static conditions showed an increase of lifetime respect to the catalysts crystallized in convection oven. This enhancement of catalyst stability is especially noticeable at the intermediate reaction temperature

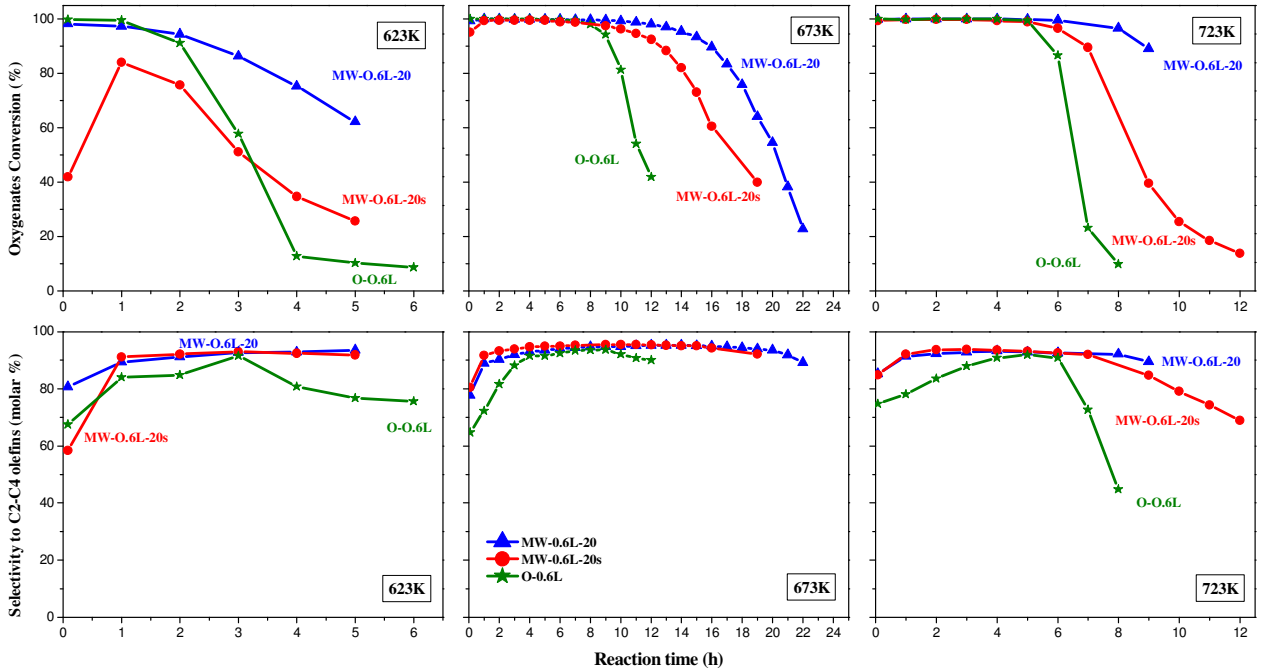

Fig. 5 Conversion of oxygenates (MeOH and DME) vs. reaction time (top) and selectivity to short chain olefins (C2–C4) vs. reaction time (bottom) for different catalysts prepared with ludox. MTO reaction test conditions: T= 623, 673 and 723 K, WHSV = 1.2 h^{-1}, 1 g of catalyst.

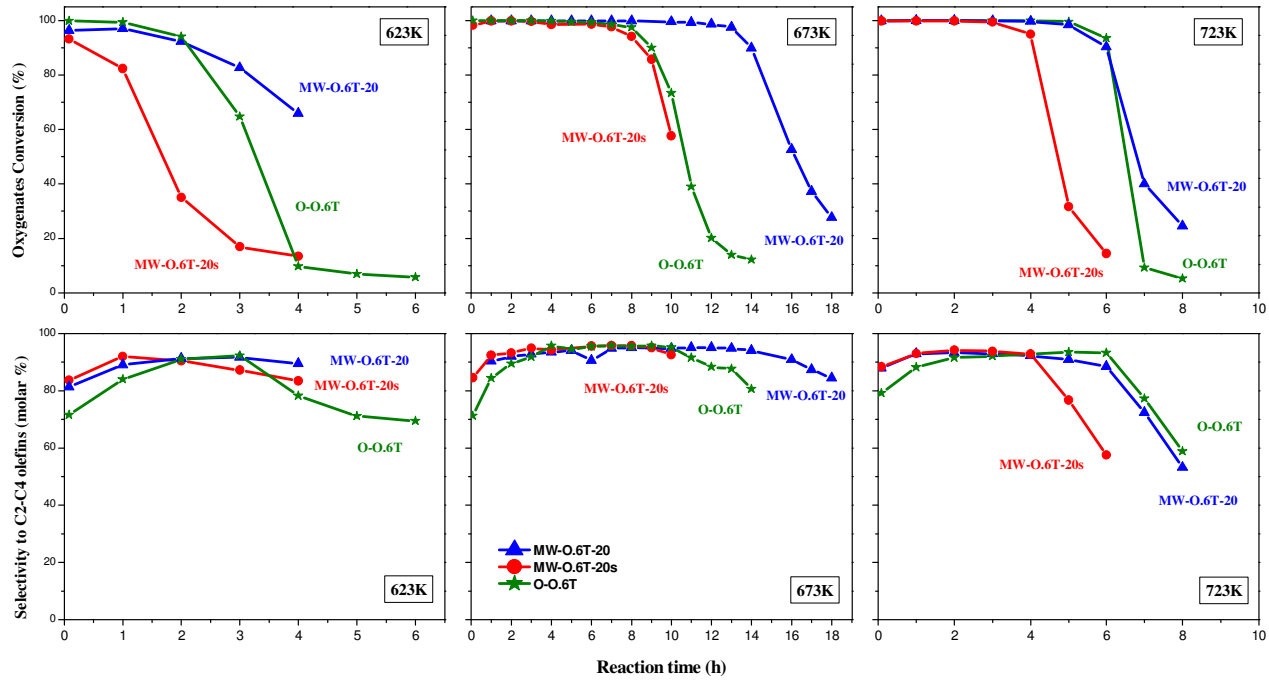

Fig. 6 Conversion of oxygenates (MeOH and DME) vs. reaction time (top) and selectivity to short chain olefins (C2–C4) vs. reaction time (bottom) for different catalysts prepared with TEOS. MTO reaction test conditions: T= 623, 673 and 723 K, WHSV = 1.2 h^{-1}, 1 g of catalyst.

Journal Name RSCPublishing

ARTICLE

(673 K), at which all catalysts showed their longest lifetime. It has been shown in previous sections that, for both silicon sources, the microwave-assisted synthesis led to catalysts with lower silicon incorporation and a concomitant lower acid sites concentration than those obtained by heating in convection oven (Table 5). The improved catalytic performance of SAPO-34 materials obtained by microwave irradiation under static conditions might therefore be attributed to their crystallite morphology. SAPO-34 crystals obtained by hydrothermal synthesis in convection oven have a rhombohedral habit while crystallization in microwave oven led to the formation of thin platelets. This change of crystal morphology leads to a significant reduction of surface area, in particular the one corresponding to micropores, for catalysts obtained by microwave irradiation as compared to those crystallized in convection oven (Table 2). The morphology of crystals obtained with microwave irradiation, consisting of platelets of a few tenths of nanometers thickness, would therefore lead to a higher fraction of micropores located near the external surface of crystals than in the case of rombohedral crystals. This involves a shorter diffusion path and, consequently, a reduction of the residence time of the hydrocarbons inside the micropores. It also implies that lower fraction of micropores would be blocked by coke deposited on the crystal surface and, hence, accessibility of the reactant molecules to micropores would be higher, therefore retaining high conversion during longer time.[25]

It is worth noting that catalysts obtained by microwave synthesis under stirring were less active than those obtained in static conditions. It has been shown that crystallization in the microwave oven under continuous stirring of the synthesis gels led to SAPO-34 catalysts with substantially lower textural properties than samples obtained in static conditions at the same crystallization time. It can be concluded that stirring hindered crystallization of SAPO-34, as shown by XRD, especially for samples synthesized with TEOS as silicon source. The shorter catalyst lifetime might therefore be attributed to this poorer crystallinity.

The selectivity to light olefins was very similar for all the samples, reaching a level around 90% at all temperatures tested. This selectivity increased slightly during the first hours of reaction at every temperature and was maintained nearly constant when the conversion was close to 100% (Fig. 5 and 6). In all cases, the decay of conversion due to catalyst deactivation was accompanied by a decrease of selectivity to light olefins and the formation of important amounts of methane and aromatics, as shown in Fig. 7 for tests carried out at 673 K. The same ethylene/propylene ratios were obtained at every reaction temperature with catalysts prepared by both convection oven and microwave heating in static conditions and using both silicon sources. This ratio was higher at higher reaction temperature and also increased with reaction time (Fig. S3 in Supplementary Information). The raise in ethylene/propylene ratio has been previously attributed to secondary reactions of oligomerization and cracking, which are favoured when the reaction temperature increases.[51,52]

As shown in Fig. 7, for all the catalysts, ethylene and propylene are the main products, indicating that all the synthesized SAPO-34 catalyst are very selective for the production of light olefins from methanol. In all the cases when the conversion decay starts the selectivity of long-chain hydrocarbon products increases. This may result from the olefin methylation-cracking route, which usually brings about the formation of hydrocarbon products heavier than propylene.[53]

The main limitation shown by this kind of catalysts in the MTO process is the rapid deactivation, attributed to the deposition of high molecular weight hydrocarbons on the pore entrances.[18,53-56] However, it is possible to optimize the synthesis of these materials to improve the catalyst lifetime.[22-24,49,57-59] At all the temperatures tested, samples prepared in the microwave oven without stirring retained high conversion during longer time than those obtained using the conventional oven heating. The main factor that could explain the best behaviour of these new materials prepared in the microwave oven compared to conventional samples is the plate-like morphology obtained using microwave irradiation, which reduces the diffusional path and therefore decreases the residence time of the hydrocarbons inside the micropores of the catalyst.

Conclusions

The synthesis of nanosized SAPO-34 employing microwave-assisted hydrothermal treatment was studied. The use of microwave irradiation causes a significant variation of the shape and size of SAPO-34 crystals compared with conventional heating. It also produces a very important shortening of crystallization time and lower level of silicon incorporation, which leads to slightly lower acidity. Catalytic MTO reaction tests over these SAPO-34 catalysts demonstrates that catalyst deactivation is strongly dependent on crystallite size. The nanosized SAPO-34 catalyst prepared in the microwave oven exhibit longer lifetime in the methanol conversion reactions compared to those prepared in the convection oven. The smaller crystal size and the specific morphology of the samples prepared by microwave irradiation play an important role in the MTO reaction, facilitating the accessibility of the reactant to the acid sites and therefore

Journal Name RSCPublishing

ARTICLE

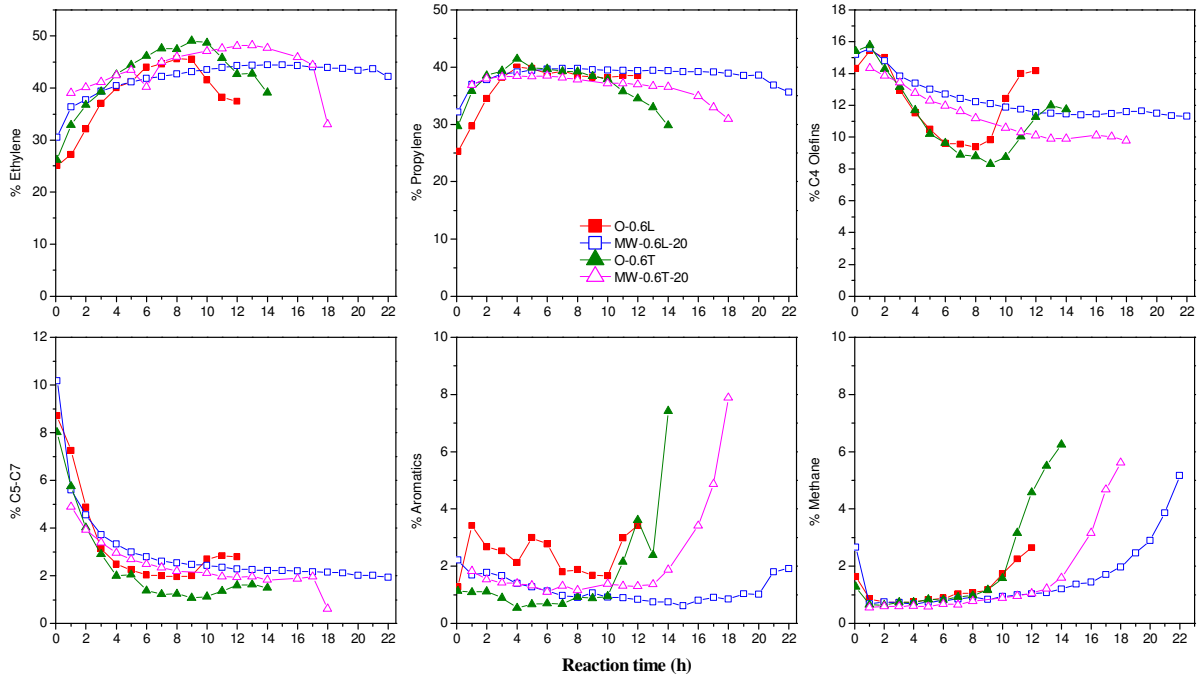

Fig. 7 Selectivities to hydrocarbon products vs. time-on-stream in the MTO reaction catalysed by SAPO-34 materials at 673 K. Tests were carried out at WHSV = 1.2 h^{-1}.

allowing to retain high conversion during longer time. It was shown that the decrease of crystal size was the main factor responsible for the improved catalytic performance in the MTO process.

Acknowledgements

We are thankful for the financial support of the Spanish Ministry of Economy and Competitiveness, project MAT2012-31127. TAM acknowledges CSIC for a JAE-PhD grant.

References

1 J. W. Park, G. Seo, *Appl. Catal. A*, 2009, **356,** 180.
2 C. D. Chang, *Catal. Rev.*, 1983, **25**, 1.
3 C. D. Chang, *Catal. Rev.*, 1984, **26**, 323.
4 C. D. Chang, A. J. Silvestri, *J. Catal.*, 1977, **47**, 249.
5 A. Gotti, R. Prins, *J. Catal.*, 1998, **178**, 511.
6 I. Wender, *Fuel Process. Technol.*, 1996, **48**, 189.
7 C. V. Ovesen, B.S. Clausen, J. Schiotz, P. Stoltze, H. Topsoe, J.K. Norskov, *J. Catal.*, 1997, **168**, 133.
8 G. A. Olah, A. Goeppert, G.K.S. Prakash, *J. Org. Chem.*, 2009, **74**,487.
9 C. Song, *Catal. Today*, 2006, **115**, 2.
10 C. N. Hamelinck, A. P. C. Faaij, *J. Power Sources*, 2002, **111**, 1.
11 S. L. Meisel, J. P. McCullough, C. H. Lechthaler, P. B. Weisz, *Chemtech*, 1976, **6**, 86.
12 M. Bjorgen, S. Svelle, F. Joensen, J. Nerlov, S. Kolboe, F. Bonino, L. Palumbo, S. Bordiga, U. Olsbye, *J. Catal.*, 2007, **249**, 195.
13 A .G. Gayubo, A. T. Aguayo, M. Olazar, R. Vivanco, J. Bilbao, *Chem. Eng. Sci.*, 2003, **58**, 5239.
14 D. Chen, K. Moljord, T. Fuglerud, A. Holmen, *Microporous Mesoporous Mater.*, 1999, **29**, 191.
15 N. Nishiyama, M. Kawaguchi, Y. Hirota, D. V. Vu, Y. Egashira, K. Ueyama, *Appl. Catal. A*, 2009, **36**, 193.
16 Y. J. Lee, H. J. Chae, S. Y. Jeong, G. Seo, *Appl. Catal. A*, 2009, **369**, 60.
17 S. C. Larsen, *J. Phys. Chem. C*, 2007, **111**, 18464.
18 D. Chen, K. Moljord, T. Fuglerud, A. Holmen, *Microporous Mesoporous Mater.*, 1999, **29**, 191.
19 A. J. Marchi, G. F. Froment, *Appl. Catal. A*, 1991, **71**, 139.
20 M. J. van Niekerk, J. C. Q. Fletcher, C. T. O'Connor, *Appl. Catal. A*, 1996, **138**, 135.
21 K. Y. Lee, H. J. Chae, S. Y. Jeong, G. Seo, *Appl. Catal. A*, 2009, **369**, 60.
22 T. Álvaro-Muñoz, C. Márquez-Álvarez, E. Sastre, *Catal. Today*, 2012, **179**, 27.
23 T. Álvaro-Muñoz, C. Márquez-Álvarez, E. Sastre, *Catal. Today*, 2013, **215**, 208.

24 T. Álvaro-Muñoz, C. Márquez-Álvarez, E. Sastre, *Catal. Today*, 2013, **213**, 219.
25 Y. Hirota, K. Murata, M. Miyamoto, Y. Egashira, N. Nishiyama, *Catal. Lett.*, 2010, **140**, 22.
26 X. Zhang, D. O. Hayward, D. M. P. Mingos, *Ind. Eng. Chem. Res.*, 2001, **40**, 2810.
27 S. A. Margolis, L. Jassie, H. M. Kingston, *J. Automat. Chem.*, 1991, **13**, 93.
28 S. H. Jhung, J. S. Chang, J. S. Hwang, S. E. Park, *Microporous Mesoporous Mater.*, 2003, **64**, 33.
29 K. Utchariyajit, S. Wongkasemjit, *Microporous Mesoporous Mater.*, 2010, **135**, 116.
30 S. C. Laha, G. Kamalakar, R. Glaser, *Microporous Mesoporous Mater.*, 2006, **90**, 45.
31 S. Mintova, S. Mo, T. Bein, *Chem. Mater.*, 1998, **10**, 4030.
32 M. Gharibeh, G. A. Tompsett, W. C. Conner, *Top. Catal.*, 2008, **49**, 157.
33 P. Chu, F. G. Dwyer, J. C. Vartuli, *US Patent 4778666*, 1988.
34 C. Gabriel, S. Gabriel, E. H. Grant, B. S. J. Halsteed, D. P. Mingos, *Chem. Soc. Rev.*, 1998, **27**, 213.
35 A. Arafat, J. C. Jansen, A. R. Ebaid, H. van Bekkum, in *Synthesis of Microporous Materials*, M. L. Occelli and H. E. Robson eds, Vol. 1, Van Nostrand Reinhold, New York, 1992.
36 A. Arafat, J. C. Jansen, A. R. Ebaid, H. van Bekkum, *Zeolites*, 1993, **13**, 162.
37 D. S. Kim, J-S. Chang, J-S. Hwang, S. E. Park, *Microporous Mesoporous Mater.*, 2004, **68**, 77.
38 C. S. Cundy, J. O. Forrest, R. J. Plaisted, *Microporous Mesoporous Mater.*, 2003, **66**, 143.
39 D. P. Serrano, M. A Uguina, R. Sanz, E. Castillo, A. Rodriguez, P. Sánchez, *Microporous Mesoporous Mater.*, 2004, **69**, 197.
40 I. Gimus, K. Jancke, R. Vetter, J. Richter-Mendau, J. Caro, *Zeolites* ,1995, **15**, 33.
41 S. H. Jhung, J.-S. Chang, J. S. Hwang, S.-E. Park, *Microporous Mesoporous Mater.*, 2004, **67**, 151.
42 J. G. Carmona, R. R. Clemente, J. G. Morales, *Zeolites*, 1997, **18**, 340.
43 C. S. Cundy, R. J. Plaisted, J. P. Zhao, *Chem. Commun.*, 1998, 1465.
44 C. S. Cundy, Collect. Czech. *Chem. Commun.*, 1998, **63**, 1699.
45 J.W. Jun, J.S. Lee, H.Y. Seok, J.-S. Chang, J.-S. Hwang, S.H. Jhung, *Bull. Korean Chem. Soc.*, 2011, **32**, 1957.
46 S. Lin, J. Yu, J. Li, R. Xu, R.P. Sharma, *Top. Catal.*, 2010, **53**, 1304.
47 F.M. Shalmani, R. Halladj, S. Askari, *Powder Technol.*, 2012, **221**, 395.
48 H. Jin, M.B. Ansari, S.-E. Park, *Adv. Porous Mater.*, 2013, **1**, 72.
49 T. Álvaro-Muñoz, C. Márquez-Álvarez, E. Sastre, *Appl. Catal. A*, 2014, **472**, 72.
50 K. S. W. Sing, D. H. Everett, R. A. W. Haul, L. Moscou, R. A. Pierotti, J. Rouquerol, T. Siemieniewska, *Pure Appl. Chem.*, 1985, **57**, 603.
51 M. Popova, C. Minchev, V. Kanazirev, *Appl. Catal. A*, 1998, **169**, 227.
52 X. Wu, M. G. Abraha, R. G. Anthony, *Appl. Catal. A*, 2004, **260**, 63.
53 J. Z. Li, Y. X. Wei, G. Y. Liu, Y. Qi, P. Tian, B. Li, Y.L. He, Z. M. Liu, *Catal. Today*, 2011, **171**, 221.
54 J. Liang, H. Li, S. Zhao, W. Guo, R. Wang and M. Ying, *Appl. Catal.*, 1990, **64**, 31.
55 A. Gronvold, K. Moljord, T. Dypvik, A. Holmen, *Stud. Surf. Sci. Catal.*, 1994, **81**, 399.
56 D. Chen, H.P. Rebo, A. Gronvold, K. Moljord, A. Holmen, *Microporous Mesoporous Mater.*, 2000, **35**, 121.
57 P. Wang, A. Lv, J. Hu, J.a. Xu and G. Lu, *Microporous Mesoporous Mater.*, 2012, **152**, 178.
58 S. Wilson, P. Barger, *Microporous Mesoporous Mater.*, 1999, **29**, 117.
59 H.-G. Jang, H.-K. Min, J. K. Lee, S. B. Hong and G. Seo, *Appl. Catal. A*, 2012, **437**, 120.